# CHARACTERISTICS OF SYNTHESIZED MAGNESIUM OXIDE NANOPARTICLES USING AQUEOUS LEAF EXTRACT OF *OROXYLUM INDICUM* (L.) AND ITS BIOACTIVITIES

Thu Zin Tun[1], Yee Mun Than[2], Ye Myint Aung[3]

## Abstract

The biological method to synthesize magnesium oxide nanoparticles with therapeutic and medicinal potential is a significant challenge in nanotechnology. In this study, to examine the efficacy of the aqueous leaf extract of *Oroxylum indicum* as stabilizing agents, they were mixed with $MgSO_4.7H_2O$ (Epsom salt) precursor solution, followed by NaOH solution to form a precipitate of magnesium hydroxide. Then, the precipitates were calcined for 5 h, to synthesize MgO NPs. Modern techniques such as XRD, SEM-EDX, FT IR, Raman, UV-visible and TG-DTA were employed to characterize the synthesized MgO NPs. The produced nanoparticles were identified as pure MgO with a cubic structure and a spherical in shape, and ranged in size from 16 to 21 nm. Furthermore, this study has reported that the synthesized MgO NPs have excellent bioactivities (antioxidant, antidiabetic, and anti-inflammatory) and revealed good results for biomedical applications.

**Keywords:** MgO NPs, *O. indicum*, green synthesis, Epsom salt, bioactivities

## Introduction

Nanotechnology can be defined as the synthesis, characterization, exploration, and application of nanosized materials for the development of science. Nanoparticles are materials with at least one dimension and an average size of 1–100 nm with an extraordinary surface area. The evolution of the "Nano" field has led to tremendous growth in various areas such as food and agriculture, pharmaceuticals, material science, biotechnology, medicine, energy, and the environment (Amrulloh *et al*., 2021). The nanoparticles are synthesized based on two approaches, namely, top-down and bottom-up, by various methods that are categorized into physical, chemical, and biological methods. Among biological methods, plants are preferred over bacteria for the green synthesis of nanoparticles because they are nonpathogenic, infinitely available, non-biohazardous, and have numerous well-studied pathways. Biomolecules present in plant extracts act as reducing and capping agents, forming stable nanoparticles. Thus, the properties of the obtained nanoparticles depend on the properties of the various phytochemicals present in the plant extracts from which they were synthesized. (Kandasamy and Prema, 2015; Zhang *et al*., 2020)

The *Oroxylum indicum* (L.) Kurz (green source) used in the present work for the environmentally friendly preparation of MgO NPs is a species of flowering plant belonging to the family of *Bignoniaceae*, has a long history of traditional medicinal uses, and modern research shows that it contains a number of medically active compounds. *Oroxylum indium* has a specific aromatic odour because of the presence of essential oils. The aromatic essential oil mainly contains phenols, fatty acids, and aldehydes. Besides oils, the plant also contains polyphenolics, flavonoids, and alkaloids (Sowjanya *et al*., 2019). The plant *O. indicum* contains a number of compounds like tannins, phenols, alkaloids, flavonoids, and saponins. The main chemical

[1] Department of Chemistry, University of Yangon
[2] Department of Chemistry, University of Yangon
[3] Department of Chemistry, University of Yangon

constituents of *O. indicum* are baicalein and scutellarein. The maximum number of phenolic compounds is present in leaf extract, followed by root, bark, and stem extract (Bhardwaj *et al*., 2018).

Magnesium oxide nanoparticles are currently popular among researchers due to their exclusive biological, electrical, and thermal properties. Magnesium oxide nanoparticles are multipurpose metal oxide nanoparticles that provide a variety of functions. In biomedical applications, there are evident reports showing MgO NPs have antioxidant, antibacterial, antifungal, and anticancer activities. In agriculture fields, they are also used in seed germination for growth, performance, chaining quality of the plant, and crop improvement, and in rice fields to increase productivity due to their antimicrobial activity. MgO NPs are also used in dietary supplements for humans and animals. In medicine, magnesium oxide is used for the relief of heartburn and sour stomach, as an antacid, as a magnesium supplement, and to improve symptoms of indigestion (Essien *et al*., 2020; Jag tap *et al*., 2021).

In this study, the synthesis, characterization, and some bioactivities of MgO NPs utilizing aqueous leaf extract of *Oroxylum indicum* by green method was closely focused and studied with modern techniques.

## Materials and Methods

### Materials

The samples of *O. indicum* leaves were collected from the plants that grow naturally around Htaw Ka Loh Village, Nyaung Done Township, Ayeyarwady Region. The commercial magnesium sulphate heptahydrate (Epsom salt) was purchased from Zi-Wa-Ka Pharmacy, Hlaing Township.

### Preparation of magnesium oxide nanoparticles

The collected fresh *O. indicum* leaves were washed using tap water, and then they were allowed to air-dry for a few weeks before being ground into powder and stored at room temperature. A dried powdered sample of *O. indicum* leaves (5 g) was weighed and mixed with 100 mL of distilled water. The mixture was then heated to 60 °C for 30 min with stirring until all the samples were evenly mixed. After heating, the solution was allowed to cool and filtered with filter paper (Whatman No. 1), and the filtrate was collected. The resulting filtrate was used for the synthesis of magnesium oxide nanoparticles (fresh extract was used for each synthesis and testing process).

Magnesium oxide nanoparticles were synthesized with the aqueous extract of *O. indicum* leaves powder using the method of Fatiqin *et al.*(2021), with slight modifications. In the synthesis process, 100 mL of *O. indicum* leaves extract solution was added dropwise by burette to $MgSO_4.7H_2O$ solution (0.2 M, 200 mL) with stirring at 600 rpm. After the two solutions were evenly mixed, 2 M NaOH was added dropwise to the mixture to get about pH 10, and then the obtained mixture was left for 3 h at 90 °C in order to optimize the formation of the magnesium hydroxide precipitate. The precipitate formed was separated from the mixture by centrifugation with a rotation of 7500 rpm at room temperature for 20 min, and the precipitate was washed three times using distilled water and once using ethanol again. The precipitate was dried in an oven to

remove any residual water and ethanol. After drying, the precipitate was ground using a mortar and pestle to form powder and calcined at 800 °C for 5 h.

**Characterization**

The green synthesized MgO nanoparticle formation was confirmed using a UV-visible spectrophotometer (UV-1800, Shimadzu). The diffraction patterns, crystalline nature and purity of MgO NPs were identified by an X-ray Diffractometer System, MultiFlex 2kW Type, Rigaku, D/max 2200, Japan. The morphological study and elemental composition of MgO NPs were performed under a scanning electron microscope equipped with an energy-dispersive X-ray (SEM-EDX) analyzer (JSM-6701F/JED 2300, JEOL, Japan). A Fourier transform infrared (FT IR) spectrometer (PerkinElmer, Spectrum Two) was employed to assess the functional groups present in MgO NPs. The crystallinity and phase identification of MgO NPs were characterized by a Raman spectrometer (PerkinElmer) to support the XRD results. To study the thermal stability of MgO NPs, a TG-DTA (DTG-60H) thermal analyzer (SHIMADZU, Japan) was used.

**Determination of antioxidant activity**

The antioxidant activity of synthesized MgO NPs was determined using the DPPH radical scavenging method using the UV-visible spectrophotometric technique. The sample solution was prepared by thoroughly mixing 1.5 mL of 20 µM DPPH solution with 1.5 mL of MgO NPs (125 to 1.95 µg/mL) in methanol and DMSO solution. Before measuring the absorbance at 517 nm against a blank, the mixture was violently mixed and allowed to stand for 30 min in the dark. The control absorbance was read without test samples. Then, the radical scavenging ability was estimated using the given formula:

$$\% \text{ RSA} = \frac{A_{\text{Control}} - (A_{\text{Sample}} - A_{\text{Blank}})}{A_{\text{Control}}} \times 100$$

**Determination of antidiabetic activity**

A test that inhibits the production of α-amylase was used to measure the anti-diabetic activity of MgO NPs. The UV-visible spectrophotometric method was used to assess the test samples' ability to inhibit α-amylase. In separate test tubes, 1 mL of the test sample solutions and 1 mL of the α-amylase solution were mixed together to make the different concentrations of the sample solutions (125 to 1.95 g/mL). Utilizing 1 mL of sodium phosphate buffer, the reaction mixture was then brought to pH 6.9. The reaction mixture was incubated at room temperature for 10 min to increase the α-amylase inhibitory activity, and then 400 µL of 1% starch solution was added. This combination was then incubated at room temperature for another 10 min. Before being heated in a water bath for 10 min at 85–90 °C, 500 µL of DNSA reagent was added. The absorbance at 540 nm was then measured after the tubes had been cooled. Without test samples, the control reading was taken.

$$\% \text{ inhibition} = \frac{A_{\text{Control}} - A_{\text{Sample}}}{A_{\text{Control}}} \times 100$$

### Determination of anti-inflammatory activity

The egg albumin denaturation inhibitory activity of the test samples was employed to study the possible mechanisms for the anti-inflammatory impact of MgO NPs using the UV-visible spectrophotometric technique according to (Naveed *et al*., 2022). The sample solution was prepared by mixing 400 µL of the test sample solutions and 300 µL of egg albumin solution in separate test tubes. The reaction mixture was then adjusted to pH 6.4 using sodium phosphate buffer (2.9 mL). To elicit the denaturation of egg albumin, the reaction mixture was incubated at RT for 20 min before being heated in a water bath for 15 min at 65–70 ℃. After that, the tubes were cooled, and the absorbance was measured at 660 nm. As a control, the solution without test samples was used. The percentage inhibition was estimated using the given formula:

$$\% \text{ inhibition} = \frac{A_{Control} - A_{Sample}}{A_{Control}} \times 100$$

## Results and Discussion

### Green synthesis of magnesium oxide nanoparticles

The synthesized MgO NPs obtained from commercial Epsom salt ($MgSO_4.7H_2O$) via phytochemicals in *O. indicum* leaf extract were white in colour, powdery, crystalline, and insoluble in water (Figure 1).

**Figure 1.** Magnesium oxide nanoparticles

### Characterization of synthesized MgO NPs

### X-ray diffraction analysis

The crystalline nature and the phase purity of the synthesized MgO NPs were analyzed by the X-ray diffractometer. Figure 2 represents the diffraction patterns of MgO NPs obtained at 800 °C. It indicated the sharp peaks with no impurities The characteristic peaks were observed at 2θ degree values of 36.94, 42.92, 62.32, 74.72, and 78.68 in the crystal planes of (111), (200), (220), (311), and (222), corresponding to the XRD patterns of MgO NPs. All peaks of the Miller indices of the MgO NP samples were matched with the International Crystal Structure Data (ICSD) no.642712 of MgO. The axial lengths of a, b, and c coordinates are 4.2128 Å. All three interaxial angles α, β, and γ of 90º suggested the formation of the perfect cubic-shaped crystal of MgO NPs. The average crystallite size of the synthesized MgO NPs was calculated by the Scherrer equation and was found to be 23.19 nm.

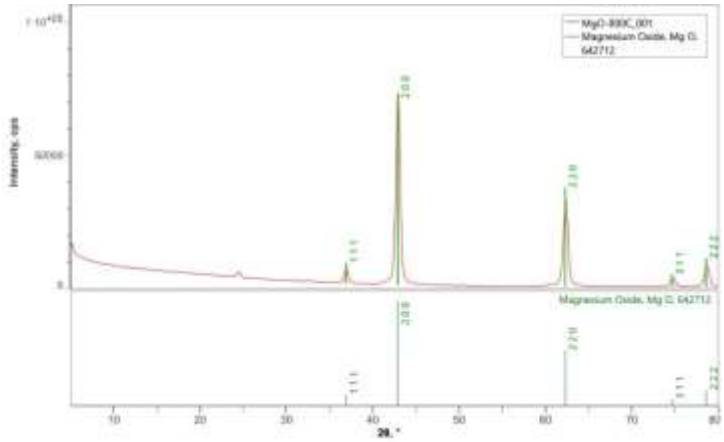

**Figure 2.** X-ray diffractogram of MgO NPs using an aqueous extract of *O. indicum* leaves

**SEM-EDX analysis**

Morphological analysis of the synthesized MgO NPs was carried out using SEM. The SEM image (Figure 3) of MgO NPs shows that the resulting MgO NPs are in the form of a spherical shape with particle sizes between 16 and 21 nm. The SEM image of MgO NPs shows good surface properties with uniform distribution of the particles however, the majority of them was clumped together. The calculated magnesium oxide nanoparticles have an average particle size of 18.5 nm in SEM images. In addition, EDX analysis confirmed the elemental composition of synthesized MgO NPs, which revealed the presence of $Mg^{2+}$ ions and $O^{2-}$ ions at high intensity with a weight ratio of 2:1 in the sample (Figure 4).

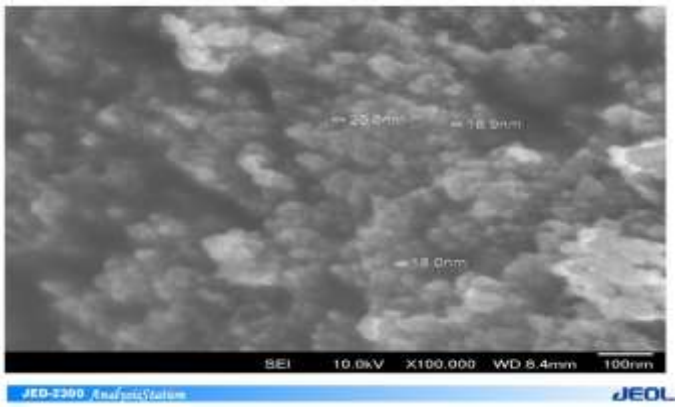


**Figure 3.** SEM image of MgO NPs using an aqueous extract of *O. indicum* leaves

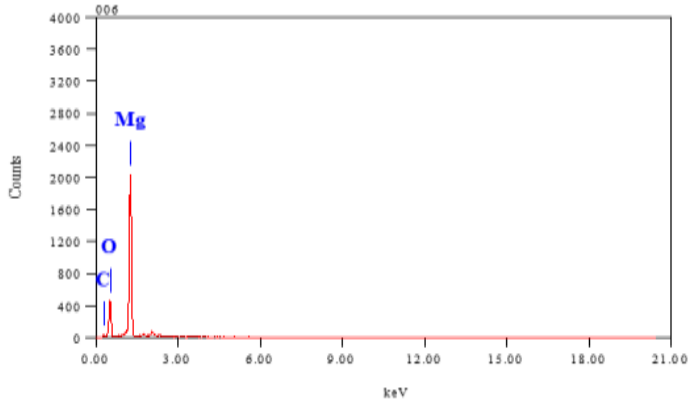


**Figure 4.** EDX image of MgO NPs using an aqueous extract of *O. indicum* leaves

## FT IR spectroscopic analysis

Figure 5 represents the FT IR spectrum of the synthesized MgO NPs using an aqueous extract of *O. indicum* leaves after calcination at 800 °C. From this spectrum, it can be observed that the main peak at 846 $cm^{-1}$ corresponds to the stretching vibration of the Mg-O bond, which indicats the formation of Mg-O linkage in MgO NPs as well as the stabilization of MgO NPs (Jeevanandam *et al*., 2020; Balakrishnan *et al*., 2020). There are no other peaks in the spectrum, indicating the influence of the Mg-O bond in the composition of MgO NPs in agreement with the SEM-EDX result.

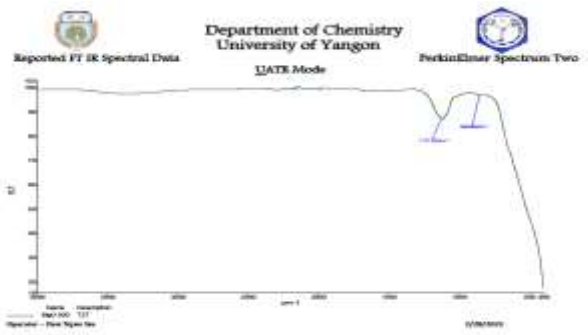


**Figure 5.** FT IR spectrum of MgO NPs using an aqueous extract of *O. indicum* leaves

## Raman spectroscopic analysis

The Raman spectrum of the synthesized MgO NPs at 800 °C was determined to support the XRD findings, and the outcomes are expressed in Figure 6. The spectrum shows strong peaks at various regions, indicating the cubic structure as designated to the tangential modes of MgO in the amorphous phase (Athar *et al.,* 2012).

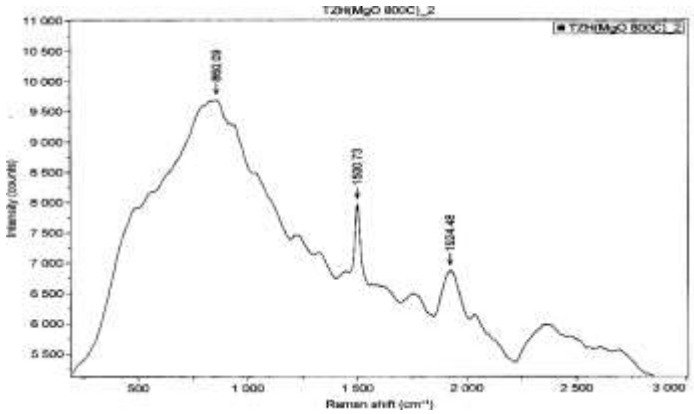


**Figure 6.** Raman spectrum of MgO NPs using an aqueous extract of *O. indicum* leaves

## UV-visible spectroscopic analysis

UV-visible absorption spectroscopy is widely used to examine the optical properties of nanosized particles. The optical properties of metal nanoparticles strongly depend on the size, shape, and interaction between the particles present on the surface of the nanoparticles. The UV-visible absorption spectrum (Figure 7) of MgO NPs showed the absorption peak at 261 nm, which confirmed the formation and stability of MgO NPs.

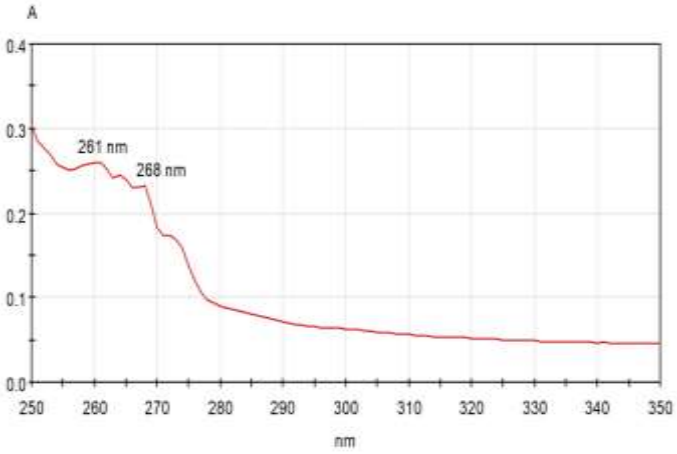


**Figure 7.** UV-visible spectrum of MgO NPs using an aqueous extract of *O. indicum* leaves

## TG-DTA thermographic analysis

TG-DTA analysis was used to assess the thermal observation of synthesized MgO NPs using an aqueous leaf extract of *O. indicum* after calcination at 800 °C. The thermogram (Figure 8) of MgO NPs indicated only one endothermic peak at 71.41 °C, which was due to the elimination of physically absorbed water from the sample surface. The absence of any other peaks indicated that no other organic constituents were left in the nanoparticles.

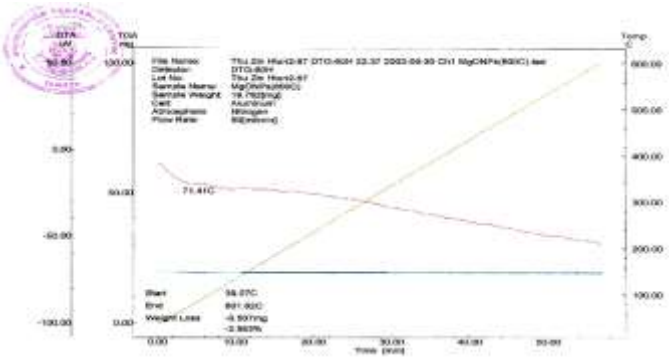

**Figure 8.** TG-DTA thermogram of MgO NPs using an aqueous extract of *O. indicum* leaves

## Screening of the Biological Properties of MgO NPs

### Antioxidant activity of MgO NPs

A change in the colour of the DPPH solution serves as a marker for the screening of antioxidant activity. The synthesized MgO NPs changed the colour of the DPPH solution from violet to light yellow, indicating that they might be antioxidants. The antioxidant activity is shown by the 50% inhibitory concentration ($IC_{50}$). The lower the $IC_{50}$ values, the higher the free radical scavenging activity, i.e., the higher the percentage of antioxidant properties. From these results, the $IC_{50}$ values of the standard ascorbic acid and the synthesized MgO NPs were observed at 1.94 µg/mL and 1.04 µg/mL, respectively. These results revealed that the synthesized MgO NPs have more potent antioxidant activity than the standard ascorbic acid, as shown in Table 1 and Figure 9.

**Table 1. Antioxidant Activity (% Inhibition) and $IC_{50}$ Values of Synthesized MgO NPs and Standard Ascorbic Acid**

| Samples | % Radical Scavenging Activity (±SD) | | | | | | | $IC_{50}$ µg/mL |
|---|---|---|---|---|---|---|---|---|
| | 62.5 µg/mL | 31.25 µg/mL | 15.63 µg/mL | 7.81 µg/mL | 3.91 µg/mL | 1.95 µg/mL | 0.98 µg/mL | |
| Ascorbic acid | 75.74± 0.001 | 75.51± 0.000 | 75.28± 0.001 | 75.06± 0.002 | 72.79± 0.001 | 50.11± 0.002 | 42.18± 0.002 | 1.94 |
| MgO NPs | 56.15± 0.003 | 54.23± 0.002 | 53.90± 0.001 | 52.25± 0.002 | 51.26± 0.001 | 50.44± 0.003 | 49.97± 0.003 | 1.04 |

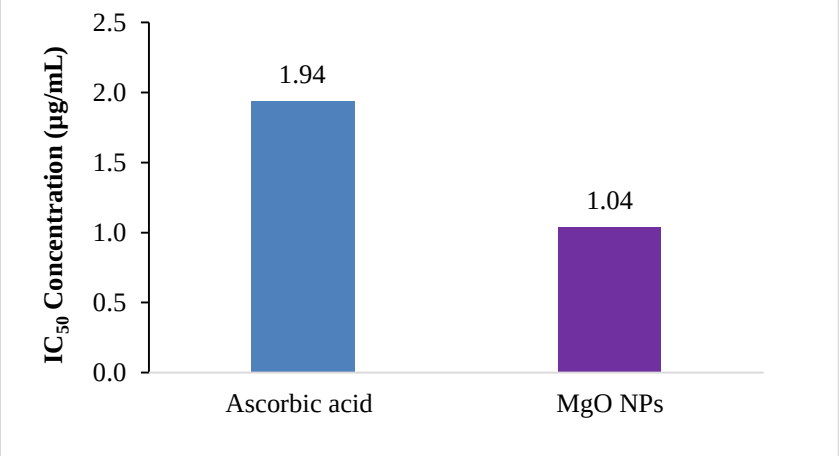


**Figure 9.** A bar graph of $IC_{50}$ values of the antioxidant activity of synthesized MgO NPs and standard ascorbic acid

**Antidiabetic activity of MgO NPs**

The antidiabetic activity of the synthesized MgO NPs using an aqueous extract of *O. indicum* leaves was assessed by using α-amylase inhibitory assay. The percentage of inhibition (42.80–59.09 %) increased with increasing the MgO NP concentration (1.95–125 µg/mL), indicating the antidiabetic effect in a dose-dependent manner. The greatest inhibition of MgO NPs was 59 %, whereas at the same dose (125 µg/mL), the common medication metformin showed 60 % inhibition. As shown in Table 2 and Figure 10, the $IC_{50}$ values of MgO NPs and the standard metformin drug were 4.78 µg/mL and 3.79 µg/mL, respectively. So, it can be seen that the green synthesized MgO NPs using the aqueous leaf extract of *O. indicum* have the potential to reduce diabetes about the same as the standard medication.

**Table 2. Antidiabetic Activity (% Inhibition) and $IC_{50}$ Values of Synthesized MgO NPs and Standard Metformin Drug**

| Samples | % α-Amylase inhibition activity (±SD) | | | | | | | $IC_{50}$ µg/mL |
|---|---|---|---|---|---|---|---|---|
| | 125 µg/mL | 62.5 µg/mL | 31.25 µg/mL | 15.625 µg/mL | 7.8125 µg/mL | 3.91 µg/mL | 1.95 µg/mL | |
| Metformin drug | 59.94± 0.000 | 59.09± 0.000 | 58.81± 0.000 | 57.39± 0.000 | 52.27± 0.001 | 50.28± 0.001 | 45.74± 0.001 | 3.79 |
| MgO NPs | 59.09± 0.001 | 55.97± 0.000 | 55.40± 0.001 | 52.84± 0.000 | 51.99± 0.001 | 49.43± 0.001 | 42.80± 0.000 | 4.78 |

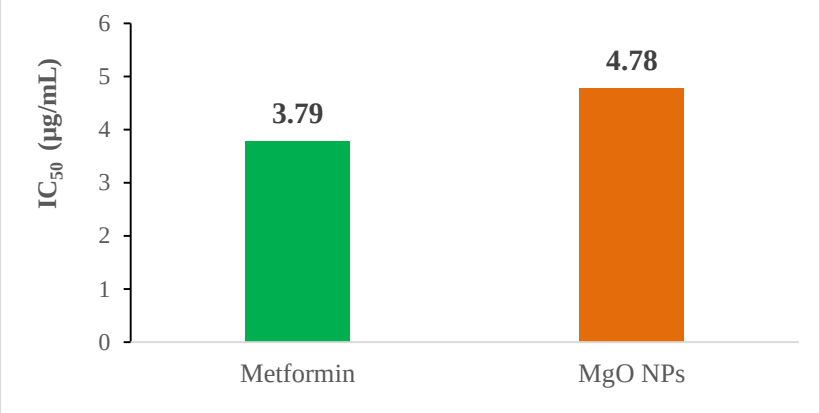


**Figure 10.** A bar graph of $IC_{50}$ values of antidiabetic activity of synthesized MgO NPs and standard metformin drug

**Anti-inflammatory activity of MgO NPs**

MgO NPs were discovered to prevent the denaturation of albumin by heat based on *in vitro* tests. When heated, the reaction mixture containing MgO NPs exhibited no cloudy appearance or precipitation, but egg albumin without MgO NPs produced white precipitation. The results were contrasted with those of diclofenac sodium, a common anti-inflammatory drug. According to the findings, the standard diclofenac sodium drug (10.56 to 84.39 %) demonstrated less inhibition than MgO NPs (34.25 to 84.57 %) at the same concentrations (1.95-125 µg/mL). The $IC_{50}$ values were found to be 4.52 µg/mL for MgO NPs and 6.77 µg/mL for standard diclofenac sodium, indicating that the synthesized MgO NPs have more effective anti-inflammatory activity than the medication (Table 3 and Figure 11).

**Table 3.** Anti-inflammatory Activity (% Inhibition) and $IC_{50}$ Values of Synthesized MgO NPs and Standard Diclofenac Sodium Drug

| **Samples** | **% Inhibition of Albumin Denaturation Activity (±SD)** | | | | | | | **$IC_{50}$** |
|---|---|---|---|---|---|---|---|---|
| | **125 µg/mL** | **62.5 µg/mL** | **31.25 µg/mL** | **15.625 µg/mL** | **7.8125 µg/mL** | **3.91 µg/mL** | **1.95 µg/mL** | **µg/mL** |
| Diclofenac sodium drug | 84.39± 0.001 | 83.84± 0.000 | 81.91± 0.001 | 76.68 ± 0.002 | 56.20± 0.001 | 33.06± 0.001 | 10.56± 0.003 | 6.77 |
| MgO NPs | 84.57± 0.000 | 83.93± 0.001 | 82.74± 0.000 | 82.00± 0.001 | 70.52± 0.000 | 46.19± 0.002 | 34.25± 0.002 | 4.52 |

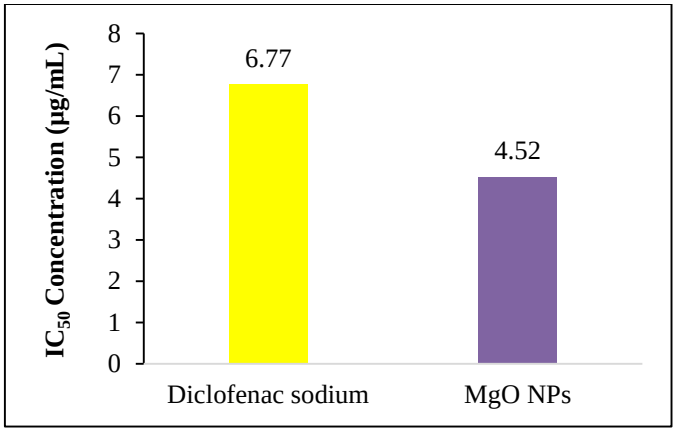


**Figure 11.** A bar graph of the $IC_{50}$ values of the anti-inflammatory activity of synthesized MgO NPs and standard diclofenac sodium drug

## Conclusion

In this investigation, an inexpensive and safe method was used for the synthesis of MgO NPs using an aqueous leaf extract of *O. indicum.* The existence of a maximal absorption wavelength at 261 nm in the UV-visible spectrum suggested the formation of MgO NPs. XRD and SEM-EDX confirmed the cubic MgO NPs with a spherical form and an average particle size of 23.19 nm by XRD and 18.5 nm by SEM. The lack of any additional functional groups using FT IR analysis indicated the higher purity of MgO NPs. The TG-DTA analysis only detected one endothermic peak at 71.41 °C, proving the purity of MgO NPs and their thermal stability. Additionally, the synthesized MgO NPs exhibited excellent antioxidant, antidiabetic, and anti-inflammatory potentials. Therefore, it can be concluded that the synthesized MgO NPs using an aqueous extract of *O. indicum* leaves have the potential to be used as an agent for biochemical applications.

## Acknowledgements

The authors would like to express their profound gratitude to the Myanmar Academy of Arts and Science for giving permission to submit this paper and to Professor and Head, Dr Ni Ni Than, Department of Chemistry, University of Yangon, for her kind encouragement. Special thanks to the Department of Chemistry, University of Yangon for providing the research facilities and to the National University of Singapore for SEM-EDX imaging.

## References

Amrulloh, H., A. Fatiqin, W. Simanjuntak, H. Afriyani, and A. Annissa. (2021). "Antioxidant and Antibacterial Activities of Magnesium Oxide Nanoparticles Prepared Using Aqueous Extract of *Moringa oleifera* Bark as Green Agents". *Journal of Multidisciplinary Applied Natural Science*, vol. 1 (1), pp. 44-53.

Athar, T., A. Hakeem, and W. Ahmed. (2012). "Synthesis of MgO Nanopowder via Non-aqueous Sol-gel Method". *Advanced Science Letters*, vol. 5, pp. 1-3.

Balakrishnan, G., R. Velavan, K. M. Batoo, and E. H. Raslan. (2020). "Microstructure, Optical and Photocatalytic Properties of MgO Nanoparticles". *Elsevier*, vol. 16, pp. 1-4.

Bhardwaj, A., A. Pathak, D. Bhatia, J. Sahoo, U. Batra, M. Tripathi, T. Mishra, and P. Choudhary. (2018). "A Phyto-pharmacological Overview on *Oroxylum indicum* (Linn.) Vent.". *International Journal of Advanced Research,* vol. 6 (8), 291-297.

Essien, E. R., V. N. Atasie, A. O. Okeafor, and D. O. Nwude. (2020). "Biogenic Synthesis of Magnesium Oxide Nanoparticles Using *Manihot esculenta* (Crantz) Leaf Extract". *International Nano Letters*, vol. 10, pp. 43-48.

Fatiqin, A., H. Amrulloh and W. Simanjuntak. (2021). "Green Synthesis of MgO Nanoparticles using *Moringa oleifera* Leaf Aqueous Extract for Antibacterial Activity". *Bulletin of the Chemical Society of Ethiopia,* vol. 35 (1), pp. 161-170.

(MgO) Nanoparticles in various domains". *Advanced Materials Lett*ers, vol. 11 (8), pp. 1-10.

Jagtap, K. R., S. R. Hore, P. S. Patil, S. A. Patil, and N. V. Awati. (2021). "Synthesis of Magnesium Oxide Nanoparticles by Using Green Method". *International Journal of Research in Engineering and Science*, vol. 9 (6), pp. 7-14.

Jeevanandam, J., Chan, Y. S., Wong, Y. J., and Hii, Y. S. (2020). "Biogenic Synthesis of Magnesium Oxide Nanoparticles using *Aloe barbadensis* Leaf Latex Extract". *IOP Conference Series: Materials Science and Engineering*, vol. 943 (12030), pp. 1-14.

Kandasamy, S., and R. S. Prema. (2015). "Methods of Synthesis of Nanoparticles and its Applications". *Journal of Chemical and Pharmaceutical Research*, vol. 7 (3), pp. 278-285.

Naveed, M., H. Batool, S. U. Rheman, A. Javed, S. I. Makhdoom, T. Aziz, A. A. Mohamed, M. Y. Sameeh, M. W. Alruways, A. S. Dablool, A. A. Almalki, A. S. Almari, and M. Alhomrani. (2022). "Characterization and Evaluation of the Antioxidant, Antidiabetic, Anti-inflammatory, and Cytotoxic Activities of Silver Nanoparticles Synthesized using *Brachychiton populneus* Leaf Extract". *Processes,* vol. 10 (1521), pp. 1-18.

Sowjanya, K., S. Swati, M. Manasa, S. Srilakshmi, and K. Mahima. (2019). "Review on *Oroxylumindicum*". *Journal of Pharmaceutical Sciences and Research,* vol. 11 (8), pp. 2905-2909.

Zhang, D., X-L. Ma, Y. Gu, H. Huang, and G-w. Zhang. (2020). "Green Synthesis of Metallic Nanoparticles and their Potential Applications to Treat Cancer". *Frontiers in Chemistry*, vol. 8 (799), pp. 1-18.